11^{th} International Conference on Fracture Mechanics of Concrete and Concrete Structures
FraMCoS-11
J. M. Chandra Kishen, A. Ramaswamy, S. Ray and R. Vidyasagar (Eds)
https://doi.org/10.21012/FC11.092397

STUDY ON INTERACTION BETWEEN FRACTURE AND CREEP OF UHSC USING MICROINDENTATION TECHNIQUE

MAHESH S.[*,†], **ANOOP M.B.**[*,†] **AND SAPTARSHI SASMAL**[*,†]

[*]Academy of Scientific and Innovative Research (AcSIR), Ghaziabad - 201002, India
[†]CSIR-Structural Engineering Research Centre (CSIR-SERC), Chennai - 600113, India
e-mail: mahesh.shankar95@gmail.com, anoop@serc.res.in, saptarshi@serc.res.in

Key words: Fracture, Creep, Creep-Fracture Interaction, Improved Energy method, Micro indentation, Cement paste, Silicafume, Microstructure.

Abstract. The interaction between fracture and creep in cementitious materials can be interpreted as the cracking that occurs during sustained loading and the effect this cracking has on subsequent change of creep. This study aims at examining creep-fracture interaction in UHSC cement paste mixes (w/b = 0.20) with varying levels of silica fume (SF) replacement (0%, 20%, and 40%) for the two different holding periods (5s and 180s) at different ages (3d, 7d, 28d, 90d) using microindentation technique. This preliminary results of a detailed experimental investigations revealed that longer dwelling time (180s) under sustained load led to decrease in fracture toughness (K_c), indicating progressive internal microcracking. This microcracking cause relaxation of stress at one site and overstressing at other site. This stress imbalance due to microcracking, influence the long-term creep rate thereby establishing an interaction between creep and fracture.

1 INTRODUCTION

Creep is defined as deformation occurring under sustained load i.e., with the passage of time, how strain varies when the stress is maintained constant. Viscoelastic behaviour of concrete (creep) is believed to be caused by cement paste. Thus characterizing creep of cement paste helps in understanding creep of concrete. However, occurrence of fracture during sustained loading is overlooked or neglected.

Interaction between creep and fracture in normal strength concrete was investigated by various researchers [1–6]. However, research on creep-fracture interaction in Ultra High Strength Concrete (UHSC), i.e., concrete with 28-day compressive strength $>$ 100MPa is scanty.

Investigations were carried out on three sets of UHSC mixes and the fracture toughness was evaluated using improved energy method (with slight modification) under two different holding conditions, namely, 5s and 180s. Fracture was assessed during the holding phase in the test protocol and it was observed that sustained load drives the crack against the resistance of the material. This is evident through the decrease in fracture toughness value during holding period. The correlation between creep modulus and the magnitude of fracture energy change provides insights into the interaction between creep and fracture during holding phase.

The analysis of the investigation suggest that an increase in creep modulus leads to a decrease in crack growth for the corresponding age at loading. Further comprehensively examining the statistical microindentation study results, this research contributes to the understanding of the long-term creep mechanism and fracture behavior in Ultra High Strength Concrete (UHSC).

2 LITERATURE REVIEW

Even though ultra high strength concrete (UHSC) has improved strength of cement paste, there exists substantial number of cracks or crack-like voids prior to the application of external loads [7]. Also redistribution of internal forces due to non uniform shrinkage and creep results in dispersed and continuous cracking [2]. Additionally to the existing problems, low water content might cause considerable self-desiccation, which may lead to autogenous shrinkage and microcracking [8]. The density of microcracks increases with increase in autogeneous shrinkage caused by self desiccation in the case of UHSC [9]. For the subsequent study, it is helpful to review some relevant characteristics of the micro-fracture and time-dependent deformation (creep).

Researchers [7, 10–13]point out that strain caused by bond microcracking have a tendency to increase creep rate. But such a phenomenon appears beyond a certain stress to strength ratio (0.7-0.9) [13, 14]. The amount of bond crack (micro crack density) that exist before applying the load determines how much, a bond crack will extend or propagate as a result of creep. In order to detect the presence of crack growth under sustained load, researchers used different methods such as acoustic emission technique [11, 14, 15].

During a basic creep test conducted by Rossi [16], significant amount of acoustic emission activity was noted when the load is held constant (i.e., following the instantaneous loading), which indicate that additional microcracks are formed. It was interesting to note that fewer acoustic events were noted in the case of high strength concrete (HSC) compared to plain concrete, but the mean width of the crack was wider [15]. This indicates rapid failure since more elastic strain energy is converted to surface crack energy without any additional load(sustained load case) [1, 17, 18].

Observations noted by Carrasquillo et al [13, 19, 20] during microcracking study of HSC indicate the same. He recognized that mortar cracks are ”unstable,” i.e., more energy is released during their creation than is necessary to cause a fracture. Without further load, the extra energy may then continue to drive the cracks. As a result, once mortar cracking begins, new cracks grow under sustained load, which is the observed material behaviour. Key factor mentioned was that all such behaviour is dominant only at higher stress to strength ratio but fails more catastrophically with fewer planes of failure without much warning of failure. A zone of microcracks always precedes a macrocrack that spreads through concrete, which causes water vapour to travel from the micropores around the microcracks to the nearby actual microcracks. As a result, the prestressing forces in the microcrack zone rises, thereby increasing the material's apparent fracture toughness [16].

Change in moisture distribution, bond breakage and restoration along with shear slip at overstressed creep sites [6, 14, 21–23] have been widely recognized as the cause of creep of cement paste. However, the role of microcracks in long-term creep of high-strength concrete (HSC) has been overlooked. Ngab and colleagues [12, 24, 25] propose that microcracks also partially cause long-term creep, while Jessy Frech-Baronet [26] suggested that plastic deformation or inelastic effects like microcracks may not play a role in long term creep mechanisms. These opinions highlight the need for further research and examination of interaction between microcracks (fracture) and creep phenomena. This paper aims to contribute to the understanding of the interrelation between creep and fracture in UHSC by analyzing the results of a statistical microindentation study.

3 THEORETICAL BACKGROUND

From the indentation test, the effective modulus or reduced modulus E_r (a relation between material modulus and indenter modulus) is obtained. This can be deduced to get E_{IT} with the help of equation (1) [27, 28]

$$\frac{1}{E_r} = \frac{1 - v_i^2}{E_i} + \frac{1 - v_{IT}^2}{E_{IT}} \tag{1}$$

where E_i - elastic modulus of indenter probe

(1141 GPa, for diamond), E_{IT} is the elastic modulus (initial tangent modulus) of material of interest. ν_i and ν_{IT} are the Poisson's ratio of the indenter probe (0.2 for diamond) and the material (0.24 for cement paste) respectively.
Energy method is useful technique to extract fracture toughness, when geometry of crack is unknown as well as multiple cracks are presented around indentation location [5]. In the classical energy method holding phase at the maximum load, during indentation cycle, has not been considered which overestimates the fracture toughness. This was taken care by the improvised energy method by considering the holding period in the test[30, 31, 32, 33]. For the purpose of modelling load versus depth (P vs h) curve:

$$\mathrm{P} = P_{\max}\left(\frac{h}{h_r}\right)^{2V_t-1}, \quad 0 \le \mathrm{h} \le \mathrm{h_l}, \text{Loading} \tag{2}$$

$$\mathrm{P} = P_{\max}\left(\frac{h-h_r}{h_{\max}-h_l}\right)^{2V_e-1}, \quad \mathrm{h_r} \le \mathrm{h} \le \mathrm{h_{max}}, \text{Unloading} \tag{3}$$

where P_{max} is maximum applied load, h_l is penetration depth when maximum load is reached. h_{max} is maximum penetration depth when P_{max} is held during holding period. h_r is residual depth after unloading process [29].

In the above equations (2), (3), the energy constants V_t and V_e are used to characterize the loading and unloading curve which is linked to the power indices by the following equations:

$$V_t = \left(\frac{m+1}{2}\right); V_e = \left(\frac{n+1}{2}\right); \tag{4}$$

where m & n are power indxes to fit the loading and unloading curve respectively. However, the values of the energy constants V_t and V_e are estimated as the ratio of refereced energy to actual energy as shown:

$$V_t = \left(\frac{U_1+U_2}{U_2}\right); V_e = \left(\frac{U_3+U_4}{U_4}\right); \tag{5}$$

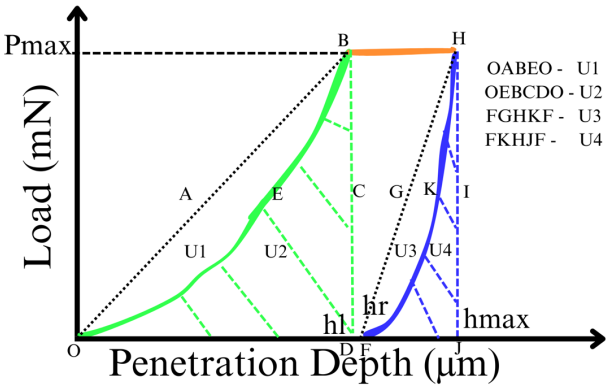

Figure 1: Concept of estimating energy constants V_t and V_e [adapted from [30, 31]]

Here, V_t and V_e are further utilized in the calculation of fracture energy. This method of estimating the constants may not be helpful in decoupling fracture energy from other energies like total, elastic and pure plastic energies. Since the loading curve comprises of fracture, V_t can be directly assumed based on the shape of indentor geometry (i.e, m = 2; V_t = 1.5 for cone [32]), instead of extracting information based on indentation curve [33–35]. V_e is elastic recovery and will not influence fracture estimation, so it is estimated as per the recommendation of improved energy method.

According to improved energy method the unknown (Pure plastic energy) which cannot be obtained directly from the experimental curve is estimated as shown below:

$$\frac{U_P}{U_t} = \frac{U_\mathrm{t} - U_e}{U_\mathrm{t}}$$

$$= \frac{1+\left(\frac{1}{2V_t}-1\right)\frac{h_r}{h_{\max}} - \frac{2}{2V_e}\left(1-\frac{h_r}{h_{\max}}\right)}{1+\left(\frac{1}{2V_t}-1\right)\frac{h_r}{h_{\max}}} \tag{6}$$

Also when no holding period is considered (i.e, h_l = h_{max}) [36] above equation condenses as follows:

$$\frac{U_P}{U_t} = 1 - \frac{v_t}{v_e}\left(1-\frac{h_r}{h_{\max}}\right) \tag{7}$$

Thus U_{crack} is estimated as shown:

$$U_{\text{crack}} = U_t - U_P - U_e \quad (8)$$

$$\Rightarrow \frac{V_t\left(1-\frac{h_r}{h_{\max}}\right)}{V_e\left[2V_t+(1-2V_t)\frac{h_1}{h_{\max}}\right]}U_t - U_e$$

$$G_c = \frac{\partial U_{crack}}{\partial A} = \frac{U_{crack}}{A_{\max}} \quad (9)$$

where G_c is critical energy release rate, U_{crack} is strain energy due to crack and A_{max} is the maximum crack area at the maximum indented depth. For the most commonly used Berkovich or Vicker's indenter, the maximum crack area is obtained by the equation A_{max} = $24.5h^2_{max}$. The fracture toughness (K_c) is then calculated by using the critical energy release rate as:

$$K_c = \sqrt{G_c E^*}, \text{in which, } E^* = \frac{E_{IT}}{1-v_{IT^2}}; \quad (10)$$

where E^* is the plane strain modulus and E_{IT} is instrumented elastic modulus of the material.

Vandamme et al. (2012) [8, 9, 10] proposed a technique to calculate creep function by conducting an indentation test. They emphasized the loading phase as the main contributor to instantaneous plasticity and derived the contact creep compliance, $L(t)$, by examining the change in depth during the subsequent holding phase, assuming no time-independent plasticity occurs during reloading and holding. The contact creep compliance function for a linear viscoelastic material is given as [22, 28, 37],

$$L(t) - \frac{1}{M_0} = \frac{\ln(t/\tau+1)}{\mathrm{C}} \quad (11)$$

where C and τ are the contact creep modulus and characteristic viscous time respectively given as,

$$\mathrm{C} = \frac{P_{\max}}{2a_c x_1}, \tau = \frac{1}{x_2}, \dot{L} = (C.t)^{-}1 \quad (12)$$

M_o is the effective modulus from equation (1) which represent the elastic modulus at the initial recovery at the onset of unloading. x_1 relates to contact creep modulus and x_2 is the reciprocal of characteristic time [37]. $\dot{L}$ is creep compliance rate and t is holding time.

With the help of two key parameters (C and τ), one can understand the creep behaviour of the material. Creep Modulus contains the long term logarithmic creep rate information [18, 22, 37, 38]. Creep modulus is inversely related to magnitude of creep. Characteristic viscous time indicate the time at which creep behaviour starts to exhibit long term logarithmic kinetics.

4 METHODOLOGY

4.1 Materials mix

In order to study the presence of interaction of creep and fracture of UHSC, cement paste was tested at various ages [28, 36, 39]. Specimen are used without being soaked in Isopropanol (IPA). Since the experiment duration is less than five minutes, hydration during that time is neglible and does not perturbate the experiment. Additionally to study interaction of UHSC when supplementary cementitious material is involved, silicafume mixes were considered. Identified silicafume mixes were SF20 and SF40, with 20% and 40% replacement of cement mass respectively. Mix proportion of PC100 consists of 100% cement, superplasticizer amounting to 0.5% of cement and no silica fume. The SF20 mix includes 80% cement, 20% silica fume, and superplasticizer(0.3% of cement). The SF40 mix contains 60% cement, 40% silica fume, and a similar amount (0.5%) of superplasticizer. The water to binder ratio is 20% (w/b = 0.2).

4.2 Surface preparation and Test protocol

A surface preparation procedure for microindentation testing using silicon carbide (SiC) papers with varying grit sizes (240 grit (30sec), 400 grit (3min), 600 grit (15min), 1200 grit (30min)) was adopted for grinding. After grinding with different grit sizes, fine polishing was carried out with the help of polishing pad and oil-based diamond suspensions of 9μm (15min), 6μm (15min), 3μm(30min) and 1μm

(30min). Each step gradually reducing surface roughness. This procedure ensures a controlled level of smoothness for accurate microindentation measurements.

The test protocol (grid size - 5x5, with interval distance of 500 μm) involved applying a force controlled maximum load of 7000 mN during the indentation test. The loading and unloading rate was set at 42000 mN/min. The loading time τ_L for each indentation was 10 seconds, followed by two different holding time τ_H of 5 seconds and 180 seconds. At the end of the holding time, the unloadingτ_U was performed in 10 seconds. The samples were tested at the age of 3, 7, 28, and 90 days.

4.3 Approach

In order to estimate the fracture energy at the beginning of the holding duration (U_{crack} at 0s instant) the unloading curve corresponding to 180s was considered to be the unloading curve at 0s. This assumption is reasonable, since the unloading curve corresponding to 180s can be considered to be the elastic unloading curve [29, 36, 40]. The effect of creep during the first instant of unloading is insignificant. By utilizing this assumption to estimate U_{crack} at 0s, the change in fracture energy can be determined and was reported.

5 RESULTS AND DISCUSSION

The following results in the tables represent the mean values of the gird area for all parameters estimated from the 25 load vs. displacement curves. Table 1 gives the mean plane strain modulus of the mixes along with coefficient of variation values in the brackets for all the three mixes considered at 3,7,28 and 90 days. Fracture toughness for two different holding time (5s and 180s) was reported in the Table 2. The % decrease in fracture energy due to crack, $\Delta U_{fracture}$) during the holding period was given in the table 3. Mean fracture energy U_{Crack} is given in the table 4. The creep modulus values are given in the table 5. Figure 2 depicts a typical load vs. displacement curve acquired using the indentation technique for 180s holding time. Dotted line represent 180s unloading curve used at 0s since it represents pure elastic recovery and less affected by creep.

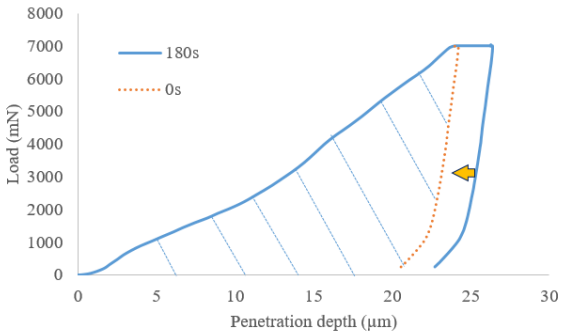

Figure 2: Typical load - displacement curve to denote change in Ucrack at 0s(shaded) and 180s.

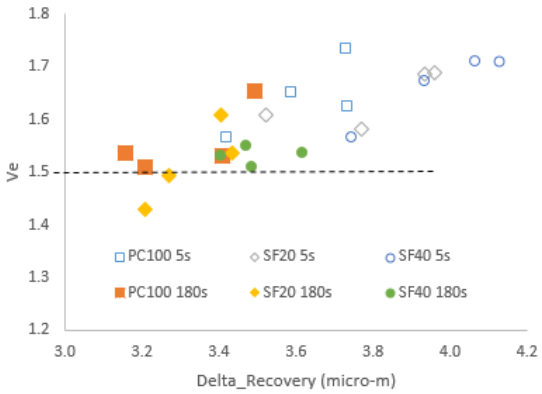

Figure 3: Mean elastic recovery energy constant V_e (5s & 180s) representing nature of unloading curve.

Table 1 shows the E^* mean plane strain modulus value (in GPa) for three different mixes (PC100, SF20, SF40) for various age at loading. Increasing trend is observed across 180s holding period for the mixes, except 90D PC100. This indicates an increase in stiffness and resistance to deformation with age due to the evolution of microstructure. Both the silicafume mixes exhibit less E^* value compared to reference mix (PC100).

5.1 Fracture

Further to understand the estimated fracture toughness (K_c), the elastic recovery en-

Table 1: Mean plane strain modulus E* (GPa) of three mixes (PC100, SF20, SF40)

Age	PC100		SF20		SF40	
(Days)	5s	180s	5s	180s	5s	180s
3	38.201(10%)	35.607(11%)	30.971(9%)	29.556(6%)	30.296(8%)	25.351(7%)
7	44.781(7%)	39.982(9%)	33.767(9%)	33.815(6%)	32.122(9%)	29.861(14%)
28	48.133(7%)	46.654(6%)	41.056(7%)	38.119(10%)	31.019(7%)	31.589(6%)
90	44.301(6%)	42.147(9%)	39.632(8%)	38.771(8%)	34.498(7%)	32.653(10%)

*Note the values in the bracket denotes coefficient of variation in percentage.

Table 2: Mean fracture toughness K_c $(MPa - m^{1/2})$ using improved energy method

Age	PC100		SF20		SF40	
(Days)	5s	180s	5s	180s	5s	180s
3	1.338 (42%)	1.275 (36%)	1.190 (49%)	0.849 (33%)	1.176 (49%)	0.596 (68%)
7	1.719 (51%)	1.399 (37%)	1.170 (29%)	1.198 (35%)	1.498 (36%)	1.089 (61%)
28	2.073 (41%)	1.791 (34%)	1.499 (57%)	1.233 (47%)	1.297 (43%)	0.985 (53%)
90	1.938(30%)	1.739(47%)	1.794(22%)	1.096(37%)	1.320(42%)	1.289(49%)

*Note the values in the bracket denotes coefficient of variation in percentage.

ergy constant V_e, which represents curvature of unloading curve, needs to be critically explored. When V_e = 1, then it indicates that the unloading curves is linear [29] representing ideal elastic behaviour. Figure 3 represents data of elastic energy constant V_e versus $\Delta_{Recovery}$. $\Delta_{Recovery}$ represents difference between h_{max} and h_r, where h_r is the final residual depth and h_{max} is maximum penetration depth (Refer figure 1). As seen in the Figure 3 at 180s holding period, for all the mixes, V_e values lie around 1.5 compared to 5s holding time. From this it is understood that almost elastic recovery occurs when load is held for 180s at early ages. Thus it is convient to use improved energy method approach for V_e. Unlike V_e, V_t should not be evaluated based on curve information which contains cracking information in order to decouple pure plastic energy. V_t is taken as 1.5 (ie., m=2 for cone geometry) directly based on the indenter geometry [32].

Average Fracture toughness (K_c) value decreases, on comparing 5s and 180s holding period for any specific age at loading (Refer Table 2). Such a trend explains that fracture toughness value decreases due to sustained loading.

Table 3: Mean Change in fracture energy due to crack $\Delta U_{fracture}$ x 10^{-07} (N-m) obtained by improved energy method

Age	PC100	SF20	SF40
(Days)	0s to 5s	0s to 5s	0s to 5s
3	1.63 (20)	1.91 (20)	3.43 (30)
7	1.84 (20)	1.75 (21)	2.57 (18)
28	1.73 (19)	1.70 (21)	2.14 (19)
90	1.59 (18)	1.72 (18)	1.55 (18)
	0s to 180s	0s to 180s	0s to 180s
3	3.13 (32)	2.10 (32)	2.40 (35)
7	3.34 (36)	2.50 (29)	3.80 (32)
28	2.49 (28)	2.60 (33)	2.70 (32)
90	2.81 (28)	1.65 (33)	2.60 (25)

*Note % decrease w.r.t. 0s is given in the bracket.

It is interesting to note that under the sustained load decrease in the fracture toughness (K_c) indicates crack growth during holding period, provided K_c is estimated through the principles of improved energy method and its as-

sumptions. At the same time creep deformation is also observed.

Energy released during localization of nano cracks due to peak load might coalesce into microcrack which might be driven without any further load and cause fracture [41]. This explains why the cement paste specimen develops microcracks over a prolonged holding period and it is evident from two different holding durations.

5.2 Creep

It is noted from Table 5 that the values of creep modulus C increase with increase in age at loading (i.e., magnitude of creep decreases with the increase in age at loading) for all mixes considered. This trend is already observed in the concrete scale [2, 14]. This is beacuse of the solidification of the hydration products which adds strength to the entire system and results in a smaller, more disconnected pore structure, in turn lowering the creep rate. Additionally the presence of capillary water in specimens considerably increases the short-term creep contribution [28]. Drop in RH cause rise in capillary suction in the capillary pores which result in internal friction of CSH sheets reducing its sliding capacity inturn affecting long term creep [18, 26]. For any given age at loading, the mean values of the contact creep modulus, C, reduces with increase in silicafume content.

5.3 Interaction of creep and fracture

Researchers [3–5, 42] have made efforts to investigate the fracture behavior that includes a holding phase. However in those studies, the creep response is subtracted or omitted [5, 39], and the fracture toughness is estimated. Therefore to understand the interaction between fracture and creep, the occurrence of fracture during the creep phase was estimated. Inorder to outline the interaction behaviour, results of change in fracture energy $\Delta U_{fracture}$ given in table 3 is utilized. For any given mixes, Mean Change in fracture energy due to crack of 180s is greater than 5s, indicating that microcracks nucleated in the intial stage might have grown or propagated during 180s holding time. Percentage decrease of $\Delta U_{fracture}$ is significant at early ages (3D & 7D) compared to later ages (28D & 90D) .This could be due to resistance offered by the evolution of the microstructure of the mixes. Addtionally it is evident from table 4 that (U_{crack})5s is quite significant compare to (U_{crack})180s indicating that energy released during first 5sec is utilized to drive the crack when holding period is increased to 180s.

Based on the table 3 and 5, it is found that with increase in creep modulus (C) there is decrease in change in crack growth $\Delta U_{fracture}$ with respect to age at loading. However, it's important to note that the at early age (3D and 7D) crack growth during creep phase is high compared to later ages (28D and 90D).

Table 4: Mean fracture energy U_{crack} x 10^{-07} due to crack (N-m) obtained by improved energy method

Age	PC100	SF20	SF40
(Days)	5s	5s	5s
3	6.558	7.874	7.960
7	7.478	6.442	11.60
28	7.556	6.392	9.250
90	7.317	8.046	7.055
	180s	180s	180s
3	6.691	4.484	4.384
7	5.947	6.166	7.852
28	6.479	5.179	5.869
90	7.225	3.278	7.596

Every time a macrocrack propagate through specimen, a zone of microcracks pre-exist , causing water vapour to flow from the neighbouring micropores to microcracks causing increase in prestressing forces in that zone, resulting in rise of fracture toughness K_c[23] [6, 16].This hypothesis may not be observed in low w/b ratio samples like UHSC. This is reflected in the trend depicted across fracture toughness value K_c(Ref Table 2 & 3). As a re-

Table 5: Mean Contact Creep Modulus C (GPa)

Age	PC100	SF20	SF40
(Days)	180s	180s	180s
3	78.910(30%)	70.827(10%)	48.731 (18%)
7	87.784(21%)	93.913(13%)	66.322 (25%)
28	157.122(11%)	95.680(32%)	73.708 (10%)
90	168.656(15%)	138.025(15%)	109.752(15%)

*Note the values in the bracket denotes coefficient of variation in percentage.

sult of disruption caused by microcracking at different times at different overstressed sites, long term creep diminishes. In other words exhaustion of overstressed creep sites and progressive relaxation of shear stress at those sites cause decline in creep rate [2, 23].This explains the two way influence or the interaction of creep and fracture in UHSC.

6 CONCLUSION

The study investigated the interrelation between creep and fracture in UHSC by analyzing microindentation test results. The following conclusions are drawn from the results:

- Fracture toughness (K_c) decreases during the holding phase. Such a decreasing trend of K_c value without any further load (only under sustained loading) indicates existence of role of microcracks during creep phase i.e, microcracks initiated in the early stages propagated during the 180s holding period.

- This crack propagation or microcrack growth cause relaxation of stress at one site and overstressing at other site. When such process progresses, non-availability of overstressed site causes decrease in long term creep rate. Thus illustrating interaction between creep and fracture.

7 ACKNOWLEDGMENTS

The authors would like to acknowledge Shri S. Gautham of AcSIR – Research scholar, CSIR-SERC, for the support received in carrying out the specimen preparation for the experiment.

REFERENCES

[1] Zdenek P Bazant. *Fracture Mechanics of Concrete Structures: Proceedings of the First International Conference on Fracture Mechanics of Concrete Structures (FraMCoS1), held at Beaver Run Resort, Breckenridge, Colorado, USA, 1-5 June 1992*. CRC Press, 2003.

[2] Zdeněk P Bažant and Milan Jirásek. *Creep and hygrothermal effects in concrete structures*, volume 225. Springer, 2018.

[3] SH Aboubakr, EM Soliman, and MM Reda Taha. Fracture toughness of synthetic csh using nanoindentation. In *CONCREEP 10*, pages 517–526. 2015.

[4] M Reda Taha, E Soliman, M Sheyka, A Reinhardt, and M Al-Haik. Fracture toughness of hydrated cement paste using nanoindentation. *Fracture Mechanics of Concrete and Concrete Structures-Recent Advances in Fracture Mechanics of Concrete*, 2010.

[5] J Němeček, V Hrbek, L Polívka, and A Jager. Combined investigation of low-scale fracture in hydrated cement assessed by nanoindentation and fib. In *9th international conference on fracture mechanics of concrete and concrete structures, fracture mechanics for concrete and concrete structures*, pages 1–6, 2016.

[6] P Rossi, N Godart, JL Robert, JP Gervais, and D Bruhat. Investigation of the

basic creep of concrete by acoustic emission. *Materials and Structures*, 27:510–514, 1994.

[7] FO Slate and KC Hover. Microcracking in concrete. *Fracture mechanics of concrete: Material characterization and testing*, pages 137–159, 1984.

[8] Knut O Kjellsen and Hamlin M Jennings. Observations of microcracking in cement paste upon drying and rewetting by environmental scanning electron microscopy. *Advanced cement based materials*, 3(1):14–19, 1996.

[9] Vincent Sicard, Raoul Francois, Erick Ringot, and Gérard Pons. Influence of creep and shrinkage on cracking in high strength concrete. *Cement and Concrete Research*, 22(1):159–168, 1992.

[10] Pu Xincheng. *Super-high-strength high performance concrete*. CRC Press, 2012.

[11] Bernard L Meyers, George Winter, et al. Relationship between time-dependent deformationand microcracking of plain concrete. In *Journal Proceedings*, volume 66, pages 60–68, 1969.

[12] Ali S Ngab, Floyd O Slate, and Arthur H Nilson. Microcracking and time-dependent strains in high strength concrete. *ACI Journal*, 78(4):262–268, 1981.

[13] Ramon L Carrasquillo, Arthur H Nilson, and Floyd O Slate. Microcracking and behavior of high strength concrete subject to short-term loading. In *Journal Proceedings*, volume 78, pages 179–186, 1981.

[14] Adam M Neville. Creep of plain and structural concrete. *(No Title)*, pages 246–255, 1983.

[15] P Rossi, JL Robert, JP Gervais, and D Bruhat. The use of acoustic emission in fracture mechanics applied to concrete. *Engineering Fracture Mechanics*, 35(4-5):751–763, 1990.

[16] P Rossi. Influence of cracking in the presence of free water on the mechanical behaviour of concrete. *Magazine of concrete research*, 43(154):53–57, 1991.

[17] Ted L Anderson. *Fracture mechanics: fundamentals and applications*. CRC press, 2017.

[18] Ya Wei, Siming Liang, and Weikang Kong. Multiscale prediction of creep property of cementitious materials. In *Mechanical Properties of Cementitious Materials at Microscale*, pages 411–463. Springer, 2022.

[19] Ramon Luis Carrasquillo. *Microcracking and engineering properties of high-strength concrete*. Cornell University, 1980.

[20] Ramon L Carrasquillo, Arthur H Nilson, and Floyd O Slate. Properties of high strength concrete subjectto short-term loads. In *Journal Proceedings*, volume 78, pages 171–178, 1981.

[21] Zhao Chen, Jessy Frech-Baronet, and Luca Sorelli. A microindentation two-fold creep model for characterizing short- and long-term creep behavior of a cement paste. *Mechanics of Materials*, 150:103559, 2020.

[22] Matthieu Vandamme and Franz-Josef Ulm. Nanogranular origin of concrete creep. *Proceedings of the National Academy of Sciences*, 106(26):10552–10557, 2009.

[23] Hailong Ye. Creep mechanisms of calcium–silicate–hydrate: an overview of recent advances and challenges. *International Journal of Concrete Structures and Materials*, 9(4):453–462, 2015.

[24] Ali Salem Ngab. *Behavior of high-strength concrete under sustained compressive stress*. Cornell University, 1980.

[25] Ali S Ngab, Arthur H Nilson, and Floyd O Slate. Shrinkage and creep of high strength concrete. In *Journal Proceedings*, volume 78, pages 255–261, 1981.

[26] J Frech-Baronet, L Sorelli, and J-P Charron. New evidences on the effect of the internal relative humidity on the creep and relaxation behaviour of a cement paste by micro-indentation techniques. *Cement and Concrete Research*, 91:39–51, 2017.

[27] wiki.anton paar.com. Instrumented indentation testing, June 2000.

[28] Shatabdi Mallick, MB Anoop, and K Balaji Rao. Early age creep of cement paste-governing mechanisms and role of water-a microindentation study. *Cement and Concrete Research*, 116:284–298, 2019.

[29] Shilang Xu, Ying Feng, Jiahan Liu, and Qiang Zeng. Micro indentation fracture of cement paste assessed by energy-based method: The method improvement and affecting factors. *Construction and Building Materials*, 231:117136, 2020.

[30] Qiang Zeng, Ying Feng, and Shilang Xu. A discussion of "application of nano-indentation methods to estimate nanoscale mechanical properties of shale reservoir rocks" by k liu, m osatadhassan and b bubach. *Journal of Natural Gas Science and Engineering*, 42:187–189, 2017.

[31] Qiang Zeng, Yongkang Wu, Yuqing Liu, and Guoping Zhang. Determining the micro-fracture properties of antrim gas shale by an improved micro-indentation method. *Journal of Natural Gas Science and Engineering*, 62:224–235, 2019.

[32] Warren Carl Oliver and George Mathews Pharr. An improved technique for determining hardness and elastic modulus using load and displacement sensing indentation experiments. *Journal of materials research*, 7(6):1564–1583, 1992.

[33] Kaushal K Jha, Nakin Suksawang, Debrupa Lahiri, and Arvind Agarwal. Energy-based analysis of nanoindentation curves for cementitious materials. *ACI Materials Journal*, 109(1):81, 2012.

[34] Kaushal K Jha, Nakin Suksawang, Debrupa Lahiri, and Arvind Agarwal. A novel energy-based method to evaluate indentation modulus and hardness of cementitious materials from nanoindentation load–displacement data. *Materials and Structures*, 48:2915–2927, 2015.

[35] MT Attaf. New formulation of the nanomechanical quantities using the β-material concept and the indentation function. *Materials Letters*, 58(6):889–894, 2004.

[36] Shilang Xu, Ying Feng, Jiahan Liu, Qiang Zeng, and Yu Peng. Microfracture characterization of cement paste at early age by indentation test. *Journal of Materials in Civil Engineering*, 30(6):04018110, 2018.

[37] Matthieu Vandamme and FJ Ulm. *The nanogranular origin of concrete creep: a nanoindentation investigation of microstructure and fundamental properties of calcium-silicate-hydrates*, volume 69. 2008.

[38] Ya Wei, Siming Liang, and Xiang Gao. Indentation creep of cementitious materials: Experimental investigation from nano to micro length scales. *Construction and Building Materials*, 143:222–233, 2017.

[39] S Gautham and Saptarshi Sasmal. Determination of fracture toughness of nano-scale cement composites using simulated nanoindentation technique. *Theoretical and Applied Fracture Mechanics*, 103:102275, 2019.

[40] Jiří Němeček. Creep effects in nanoindentation of hydrated phases of cement pastes. *Materials Characterization*, 60(9):1028–1034, 2009.

[41] Jacqueline Saliba, Frédéric Grondin, and Ahmed Loukili. Coupling creep and damage in concrete under high sustained loading. In *Framcos-7*, 2010.

[42] Eslam M Soliman, Sherif H Aboubakr, and Mahmoud M Reda Taha. Estimating fracture toughness of c–s–h using nanoindentation and the extended finite element method. *International Journal of Advances in Engineering Sciences and Applied Mathematics*, 9:154–168, 2017.